Available online at www.elixirpublishers.com (Elixir International Journal)

Bio Diversity

Elixir Bio Diver. 44 (2012) 7138-7142

ISSN: 2229-712X

Estimation of ambient radon gas concentration and its potential health effect at some faulted areas in Accra, Ghana

Akwasi B. Asumadu-Sakyi, Osborne C. Oppon and Frank K. Quashie
Nuclear Application Centre, Ghana Atomic Energy Commission, Legon- Accra, P.O.Box LG80, Ghana.

ARTICLE INFO

Article history:
Received: 29 January 2012;
Received in revised form:
17 February 2012;
Accepted: 27 February 2012;

Keywords
Radon gas,
Fault lines,
Alpha track detectors,
Ghana.

ABSTRACT

Alpha track detectors has been used for soil radon gas measurements at some faulted areas in Accra, Ghana aiming to advice the public on indoor radon gas. This was performed on forty two (42) sample pits within a 70 m X 100 m spaced grid at Dome-Kwabenya, District and fifteen (15) sample pits within a 300 m X 200 m spaced grid at Dunkonah, Weija district. Comparison method for determining uranium concentration with track-etch detectors was used for uranium levels at study areas. Soil radon gas which gets to the surfaces was estimated by monitoring radon gas 1 meter above sample pits. In the Districts, soil radon concentrations varied from 10.21 ± 0.46 kBq/m^3 to 22.67 ± 0.68 kBq/m^3 and 6.46 ± 0.36 kBq/m^3 to 27.54 ± 0.75 kBq/m^3 respectively. The estimated ambient radon gas concentration also varied from 575.97 to 1256.40 Bq/m^3 and from 376.47 to 1470.80 Bq/m^3. The ambient levels yielded an estimated annual absorbed dose varying from 10.90 to 23.77 mSv/y and from 7.12 to 28.34 mSv/y. The estimated effective dose was from 26.16 to 57.06 mSv/y and from 17.10 to 68.02 mSv/y.

Introduction

Several research in the World have delineated the relationship between fault lines and radon level where Rn-222 gas have been used as tracers of these fault lines (Chyi et al., 2002; Matsumoto et al., 2005; La Delfa et al., 2008; Ramola et al., 2007; Erees et al., 2006). This is because radon gas can migrate long distance through fractured rocks due to its half-life of 3.8235 days. Therefore high radon gas concentration in faulted areas is used as a tool for mapping fault lines. Rn-222 is an odorless, colourless inert gas which forms part of the U-238 decay series. It occurs in rocks because of the presence of uranium and radium (which is it's direct parent nuclide). Levels of radon in our houses are affected by the type of bedrock under dwellings, house foundation characteristics, radon dissolved in artesian water, ventilation and degree of air movements in living spaces. This gas does not pose much treat to human lungs because of it chemical inertness and low solubility in body fluids. Rather, the immediate daughter with their short half-life decays depositing all their energy to the respiratory tract. Also their positive charge nature aids them to attach readily to dust particles which follow then into the respiratory tract. This transforms the basal cell of the epithelial layer which leads to lung cancer (Tomášek et al; 2001; M. Abd El-Hady, 2006; http://books.nap.edu/catalog/5499.html; ICRP, 1991). Rn-222 gas measurements in Ghana started in 1976 till date by Ghana Atomic Energy Commission. These include offices, homes, mines and soil radon gas monitoring (Andam et al., 2007; Oppon et al., 1990). Studies on soil radon gas measurements at faulted Areas have also been conducted in areas in Kumasi, Accra and other regions in Ghana (Amponsah et al., 2008). Such works are necessary to establish permits for building at faulted areas as done in Europe and also to advice inhabitant on mitigation measures to reduce radon gas levels.

Tele:
E-mail addresses: pekyepe@gmail.com

Study Area

The studied areas geology fall within the Togo formation and Dahomeyan formation of Ghana as shown in Figure 1. The Togo formation are rocks forming the Akuapim range of hills trending northeast wards from the coast west of Accra through Kpong, Anim into the Republic of Togo. The mostly found rocks are phyllites, schists and quartzites whiles in some places unaltered shale and sand stone are common.

The Dahomeyan formation also occurs as four alternate belts of acid and basic gneisses trending (SSW) to (NNE) from the coastal plains east of the Togo formation. The basic gneiss is flat forming the Accra plains whiles the acid gneiss gives rise to gently undulating topography.

Common rocks are quartz, schists, metamicrogabbros forming dykes and sills. These may be massive, black and coarse crystalline. Orthogneiss and augen gneiss of dioritic to granodioritic composition occurs more especially at Otiribi and Danfa near Dodowa. The rocks consist mainly of feldspar and amphibolites and have clear foliation which gives it gneiss character (Kesse, 1985).

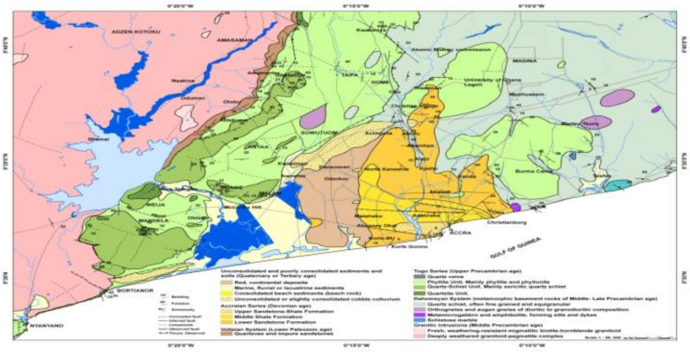

Figure 1. Geological map of the Greater Accra Metropolitan Area (GAMA) (after Muff and Efa, 2006)

Materials and Methods

Soil radon gas measurements

Soil radon gas monitoring was conducted over a study area of about 1.73 acres according to a 70 m X 100 m spaced grid of 42 sampling pits at Kwabenya and about 14.83 acres at Weija, according to a 300 m X 200 m spaced grid of 15 sampling pits. Cellulose nitrate LR-115 type II (strippable) alpha particle detectors produced by Kodak Pathé of France were used for the measurements. The detectors were cut into a dimension of 2 cm X 2.5 cm^2 and attached to the bottom of wooden stoppers with the aid of masking tape. These was then fixed into a polyvinyl chloride plastic tube (PVC) of length 25 cm and diameter of 4.5 cm and placed in holes of 75 cm depth at the various grid points as shown in Figure 2. Plywood painted with creosote and soil was used to cover the holes to prevent rain and foreign material. The detectors were then exposed for 2 weeks interval for a period of 12 weeks due logistic constraint. The detectors were detached from the wooden stoppers and etched in a 2.5 M NaOH solution for a period 90 minutes at a temperature 60 ^oC. They were then stored in a water bath to stop etching and its backing were peeled. This was followed by air drying. The spark counter in conjunction with the microfiche reader and a tally counter were used to count the registered alpha tracks. Three counts were made for each detector and the average was calculated. The track density was calculated using the average number of sparks and the Area of electrode as shown equation (1).

$$Track\ density\ (\rho) = \frac{Average\ number\ of\ counts}{Area\ of\ electrode} \quad (1)$$

The radon gas concentration was calculated using equation (2)

$$Concentration\left(\frac{kBq}{m^3}\right) = \frac{Track\ density\ (\rho)}{Calibration\ factor\ (\varepsilon) \times Exposure\ time\ in\ hours\ (T)} \quad (2)$$

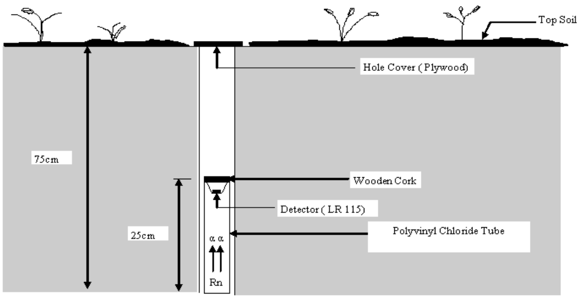

Figure 2. A Schematic diagram showing soil radon monitoring using SSNTD

Determination of Uranium Content

Soil samples were randomly collected and air dried for a period of one week. They were oven dried for a period of 24 hours at a temperature of 105 ^oC. It was then allowed to cool to room temperature. Debris was removed by sieving and the soil was grounded. 2.0 grams of the soil samples and Uranium ore standard (Pitche Blende) S-13 were packed into a rabbit capsule containing LR-115 type II alpha particle detector of dimension 2 × 3 cm^2. The packaging was performed thrice for each sample to reduce error. This was followed by 10 seconds of neutron irradiation using the Miniature Neutron source reactor at GHARR-1 centre at a flux of 5×10^{11} n/cm^2s. After one week of activity cooling, the detectors were removed and etched in a 2.5 M NaOH solution at a temperature of 60 ^oC for a period of 90 minutes. At a magnification of 400 X the optical microscope was used to evaluate the tracks formed on the detectors. Using comparison method, the uranium concentration was calculated using equation (3).

$$C_x(U) = \frac{\rho_x}{\rho_s} \bullet C_s(U) \quad (3)$$

Where C is the Uranium concentration expressed in percentage fraction, s and x refer to the standard and the unknown, ρ is the track density calculated from the counts obtained (Fleischer et al; 1975, Oppon and Aniagyei, 1988).

Correlation between concentration of soil radon gas and ambient radon gas concentration

Radon gas was monitored 1 meter above the sample pits only at Weija district due to logistics constraints for a period of three months. The radon samplers used for the soil radon gas measurement was attached unto a 1 meter stick with the aid of a cellotape and placed just above the sample pits at various grid points without changing the detectors. Due to some challenges at the study area not all the detectors were recovered after the measurement period. After the monitoring period, the detectors were detached from the wooden stoppers followed by chemical etching. Track evaluation procedure was done using the spark counter in conjunction with a tally counter and a microfiche reader. The evaluation was performed thrice for each detector and the mean was calculated to minimize error. The track density and the ambient radon concentration were calculated using the formulae in the soil radon gas measurement section. Using the equation relating the soil radon gas concentration and ambient radon gas concentration as in Figure 3, the ambient radon gas concentration was estimated.

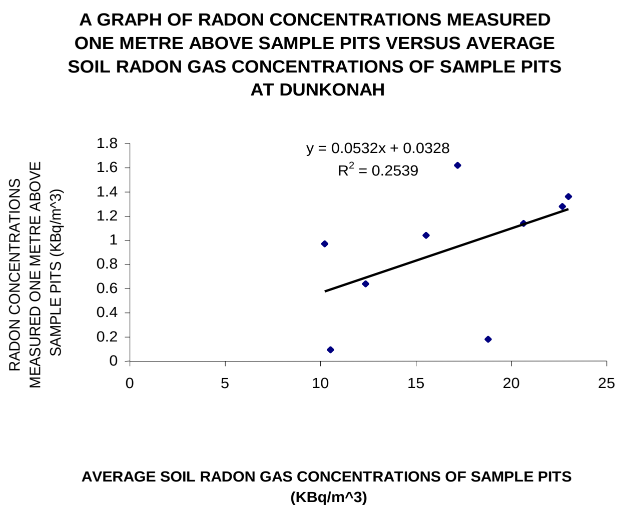

Figure 3. A graph of radon concentrations measured one meter above sample pits versus average soil radon gas concentrations of sample pits at

Determination of estimated annual absorbed dose and annual effective dose

Using the ambient radon gas concentrations obtained at both studied areas, the annual effective doses indoors and annual absorbed dose in the air was calculated. The annual effective dose was calculated using equation (3).

$$E\left(mSv\,y^{-1}\right) = D_{Rn} \bullet W_R \bullet W_T \quad (3)$$

Where D_{Rn} - Annual Absorbed Dose

W_{Rn} - Radiation weighting factor for alpha particles (20) (ICRP, 1991)

W_T - Tissue weighting factor for the lung (0.12) (ICRP, 1991)

But in calculating D_{Rn}, a value of 9.0×10^{-6} mSv h^{-1} per Bqm^{-3} was used for the conversion factor (effective dose received by adults per ^{222}Rn activity per unit of air volume) and also a 0.8 equilibrium factor for ^{222}Rn outdoor. An occupancy factor of 0.3 was assumed based on the period farmers spend on their farms, that is

$$\frac{8\ hrs}{24\ hrs} = 0.333 \cong 0.3$$

Therefore for a calculated radon concentration, the annual absorbed dose was calculated using the equation (4).

$$D_{Rn}\left(m\,Sv\,y^{-1}\right) = C_{Rn} \bullet D \bullet F \bullet T \qquad (4)$$

Where C_{Rn} – Rn-222 concentration

F- Rn-222 equilibrium factor outdoor (0.8)

T-Indoor Occupancy time

$\left(0.3 \times 24\,hrs \times 365\,days = 8760\ \ h\,y^{-1}\right)$

D- Dose conversion factor $\left(9.0 \times 10^{-6}\ m\,Sv\,h^{-1}\ per\ Bqm^{-3}\right)$

Results and Discussions

The average soil radon gas concentrations are graphically presented in Figure 4 and Figure 5.

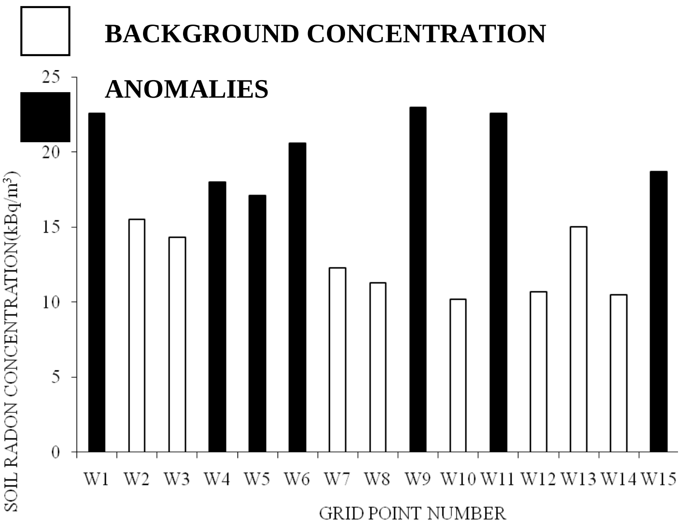

Figure 4. A bar chart of average soil radon gas concentrations against grid point locations at Weija

Figure 5. A bar chart of average soil radon gas concentrations against grid point locations at Kwabenya

The average soil radon gas concentrations at Weija district was between 10.21 ± 0.46 kBq/m^3 to 23.00 ± 0.0.69 kBq/m^3 and that of Dome-Kwabenya district was 6.46 ± 0.4 kBq/m^3 to 27.5 ± 0.75 kBq/m^3. Table 3 and 4 are estimated ambient radon gas concentration, annual absorbed dose and annual effective dose at the studied areas. The estimated ambient radon levels are graphically represented in Figure 7 and Figure 8.

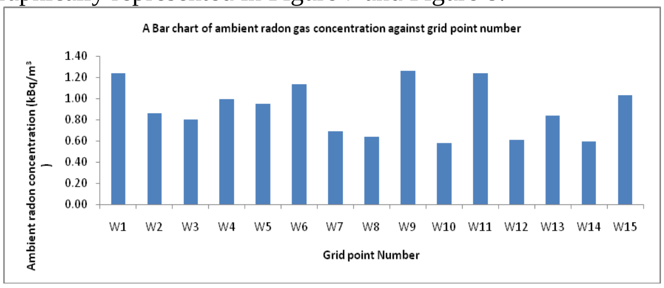

Figure 6. A bar chart of estimated radon gas concentrations against grid point locations at Weija district

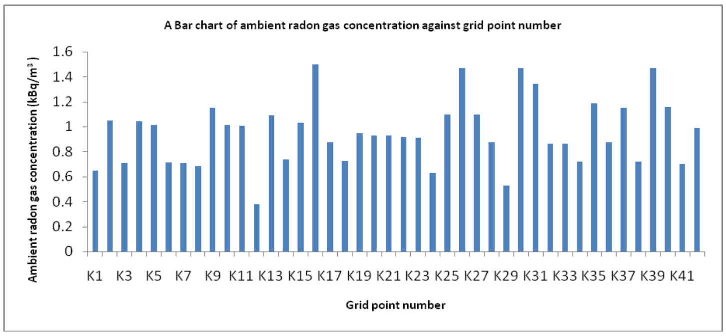

Figure 7. A bar chart of estimated radon gas concentrations against grid point locations at Dome-Kwabenya district

The soil radon values obtained at both studied areas are comparable to measurement made by (Amponsah et al., 2008) at some faulted areas in southern Ghana. Variations in soil radon gas concentration obtained may be due to difference in the geology of the underlying bedrock (Ciotoli et al; 1998). Using the mean of the average soil radon concentration as background levels and those above the background as abnormal, 46.67 % of the sample pits registered abnormal concentration at Weija and 47.61 % at Dome-Kwabenya.

For the uranium 235 concentration measurement, an average value of 0.02 % was attained at both studied areas. According to Kesse, 1985 this percentage fraction of U-235 obtained is not within the low grade uranium percentage of 0.03 – 0.05 % found in sedimentary formation that can be mined in Ghana. The high anomalies in radon gas concentration may therefore be attributed to the presence of fractured rocks which serve as vent for diffusing soil radon gas to the earth surface and also due to high out gassing rate at faulted zones (Khan et al., 1990; King et al., 1996; Baubron et al., 2002; Reddy et al., 2006). The estimated ambient radon gas concentration at Weija ranged from 575.97 to 1256.40 Bq/m^3 and that of Dome-Kwabenya was between 376.47 to 1470.80 Bq/m^3. The estimated annual absorbed dose at Weija ranged from 10.90 to 23.77 mSv/y and from 7.12 to 28.34 mSv/y at Dome-Kwabenya. The estimated effective dose at Weija also ranged from 26.16 to 57.06 mSv/y and from 17.10 to 68.02 mSv/y at Dome-Kwabenya. These studied areas are used for farming by the local community. Therefore these farmers and individuals who use the land for any purpose is exposed to these high concentrations of ambient radon gas concentration. These farmers' falls under the general public exposure, who are considered to be anyone who is not occupationally exposed or someone knowingly and voluntarily helps (other than in their employment) in care, support or comfort of a patient. The exposure to the general public is restricted by application of dose limits and the constrained optimization of radiation protection. According to the dose limits stated, the effective dose should not exceed 1 mSv in a year (W.H.O, 2009; http://www.rpop.iaea.org; http://www.dec.ny.gov/regs/4360.html). The estimated effective dose obtained is at least 20 × than the permissible dose. The results obtained for the various measurements and estimation are alarming, though ambient radon gas concentration is readily affected by air dilution and seasonal variations. Wet season inhibits radon transport whiles dry season in which the study was conducted enhances radon transport (Moreno et al., 2008).

Conclusion

This preliminary studies result at these faulted areas show that individuals who make use of the land like the farmers in such areas are being exposed to the risk of ionizing radiations by inhalation of these radon gas and its daughters which are deposited in the respiratory system. Therefore governmental bodies in charge of environmental and radiation issues should advice the local population on this ambient radon gas levels at faulted areas in Ghana.

I would recommend that Environmental protection agency (E.P.A), Ghana health services in collaboration with Ghana atomic energy commission carry out a thorough study on ambient radon gas concentration and the risk of lung cancer at faulted areas in Ghana.

Acknowledgement

Glory be to God for his guidance through this work. Also we extended our gratitude to anyone who contributed to this work and all members of the physics department.

References

Chyi LL, Chou, CY, Yang, FT, Chen, CH. Automated radon monitoring of seismicity in fault zone. Geofisica Internacional. 2002; 41(4):507-511.

Matsumoto H, Mikada, H. Fault geometry of the 2004 off the Kii peninsula earthquake inferred from offshore pressure waveforms. Earth Planets Space. 2005; 57: 161–166.

La Delfa S, Agostino I, Morelli, D, Patane, G. Soil radon concentration and effective stress variation at Mt. Etna (Sicily) in the period January 2003–April 2005. Radiat. Meas. 2008; 43: 1299 – 1304.

Ramola, RC, Choubey, VM, Negi, MS, Prasad, Y, Prasad, G. Radon occurrence in soil–gas and ground-water around an active landslide. Radiat. Meas. 2007; 43: 98 – 101.

Erees, FS, Aytas, S, Sac, MM, Yener, G, Salk M. Radon concentrations in thermal waters related to seismic events along faults in the Denizli Basin,Western Turkey. Radiat. Meas. 2006; 42: 80 – 86.

Tomášek , L, Kunz, E, Müller, T, Hůlka, J, Heribanová, A, Matzner, J, Plaček,V, Burian, I, Holeček, J, et al. Radon exposure and lung cancer risk- Czech cohort study on residential radon. The science of the Total Environment. 2002; 272: 43-51.

Abd El-Hady M, Measurement of individual radon progeny in Egyptian underground coal Mine and Related Lung Doses. Egypt. J. Solids. 2006; 29(20).

http://books.nap.edu/catalog/5499.html.

International Commission on Radiological Protection. (1991). Recommendations of the International Commission on Radiological Protection, ICRP Publication 60. Annals of the ICRP 21 Pergamon Press, Oxford.

Andam AB, Amankwah EA, Addison ECK, Nani EK. Radon measurements in Ghana: health risk assessment at the lake Bosomtwi Basin. Ghana Journal Science. 2007; 9(2): 85-93.

Oppon, OC, Aniagyei, HM., Kyere, AWK, editors. Monitor-ing of background radiations in some Ghanaian Homes Paper. International Conference on high levels of Natural Radiation; 1990 Nov 3-7; Ramsar, Islamic Republic of Iran.

Amponsah, PE, Banoeng-Yakubo, B, Andam, A, Asiedu, D. Soil radon concentration along Fault Systems in parts of South Eastern Ghana. Journal of African Earth Sciences. 2008; 51: 39–48.

Kesse, GO, The mineral and rock resources of Ghana. In: Balkema, AA, editor. The republic of Ghana – Geography, physiography, geology and geohydrology. Boston:Rotterdam; 1985. Boston. p. 9 – 45.

Fleischer, LR, Price, PB, Walker, RM, Nuclear Track in Solids. Elemental Mapping and Isotopic Analysis. University of California Press, MI; 1975. p. 489-495.

Oppon, OC, Aniagyei, HM. Report on the application of nuclear track detectors in mineral exploration: uranium. National Nuclear Research Institute, Ghana Atomic Energy Commission, Ghana. 1988.

Ciotoli, G, Etiope, G, Guerra, M, Lombardi, S. The detection of concealed faults in the Ofanto Basin using the correlation between soil-gas fracture surveys. Tectonophysics. 1998; 301: 321- 332.

Khan, HA, Tufail M, Qureshi, AA. Radon sig-nals for earthquake prediction and geological prospection. Journal of Islamic Academy of Science. 1990; 3(3): 229-231.

King, CY, King, BS, Evans, WC, Zhang, W. Spatial radon anomalies on active faults in California. Appl. Geochem. 1996; 11: 497 – 510.

Baubron, JC, Rigo, A, Toutain, JP. Soil gas profile as a tool to characterise active tectonic areas: the Jaut Pass example (Pyrenees, France). Earth Planet. Sci. Lett. 2002; 196: 69-81.

Reddy, DV, Sukhija, BS, Nagabhushanam P, Reddy, GK, Lachassagne, P, Kumar, D. Soil gas radon emanometry: A tool for delineation of fractures for ground water in granitic terrains, Journal of Hydrology. 2006; 329:186 – 195.

World Health Organization. WHO Handbook on Indoor Radon. A Public Health Perspective. WHO Press, Switzerland. 2009.

http://www.rpop.iaea.org

http://www.dec.ny.gov/regs/4360.html

Moreno, V, Baixeras, C, Font, LI, Bach, J. Indoor radon levels and their dynamics in relation with the geological characteristics of La Garrotxa, Spain. Radiat. Meas. 2008; 43: 1532–1540.

Table 3. Estimated Ambient Radon Gas Concentration, Annual Absorbed Dose and Effective Dose at Weija, District

Grid point	Average soil radon gas concentration (kBq/m^3)	Estimated Ambient radon gas concentration (Bq/m^3)	Estimated Annual Absorded dose (mSv/y)	Estimated Effective Dose (mSv/y)
W1	22.67 ± 0.68	1238.84	23.44	56.26
W2	15.54 ± 0.56	859.53	16.26	39.03
W3	14.38 ± 0.54	797.82	15.10	36.23
W4	18.01 ± 0.61	990.93	18.75	45.00
W5	17.18 ± 0.59	946.78	17.91	42.99
W6	20.64 ± 0.65	1130.85	21.40	51.35
W7	12.36 ± 0.50	690.35	13.06	31.35
W8	11.30 ± 0.48	633.96	12.00	28.79
W9	23.00 ± 0.69	1256.40	23.77	57.06
W10	10.21 ± 0.46	575.97	10.90	26.16
W11	22.63 ± 0.68	1236.72	23.40	56.16
W12	10.77 ± 0.47	605.76	11.46	27.51
W13	15.09 ± 0.56	835.59	15.81	37.95
W14	10.52 ± 0.46	592.46	11.21	26.90
W15	18.79 ± 0.62	1032.43	19.54	46.88

Table 4. Estimated Ambient Radon Gas Concentration, Annual Absorbed Dose and Effective Dose at Kwabenya, District.

Grid point	Average soil radon gas concentration (kBq/m^3)	Estimated Ambient radon gas concentration (Bq/m^3)	Estimated Annual Absorded dose (mSv/y)	Estimated Effective Dose (mSv/y)
K1	11.51 ± 0.48	645.13	12.21	29.30
K2	19.04 ± 0.63	1045.73	19.79	47.49
K3	12.70 ± 0.51	708.44	13.40	32.17
K4	18.95 ± 0.62	1040.94	19.70	47.27
K5	18.40 ± 0.61	1011.68	19.14	45.94
K6	12.83 ± 0.51	715.36	13.54	32.49
K7	12.65 ± 0.51	705.78	13.35	32.05
K8	12.25 ± 0.48	684.50	12.95	31.08
K9	20.99 ± 0.66	1149.47	21.75	52.20
K10	18.44 ± 0.62	1013.81	19.18	46.04
K11	18.32 ± 0.61	1007.42	19.06	45.75
K12	6.46 ± 0.36	376.47	7.12	17.10
K13	19.91 ± 0.64	1092.01	20.66	49.59
K14	13.25 ± 0.52	737.70	13.96	33.50
K15	18.74 ± 0.62	1029.77	19.48	46.76
K16	27.54 ± 0.75	1497.93	28.34	68.02
K17	15.87 ± 0.57	877.08	16.60	39.83
K18	13.04 ± 0.46	726.53	13.75	32.99
K19	17.17 ± 0.59	946.24	17.90	42.97
K20	16.85 ± 0.59	929.22	17.58	42.20
K21	16.82 ± 0.58	927.62	17.55	42.13
K22	16.58 ± 0.58	914.86	17.31	41.55
K23	16.47 ± 0.58	909.00	17.20	41.28
K24	11.25 ± 0.48	631.30	11.95	28.26
K25	20.02 ± 0.64	1097.86	20.77	49.86
K26	27.02 ± 0.74	1470.80	27.82	66.77
K27	20.00 ± 0.64	1096.80	20.75	49.81
K28	15.85 ± 0.57	876.04	16.58	39.78
K29	9.27 ± 0.44	524.96	9.95	23.88
K30	27.03 ± 0.74	1470.80	27.83	66.79
K31	24.65 ± 0.71	1344.18	25.43	61.04
K32	15.59 ± 0.57	862.19	16.31	39.15
K33	15.59 ± 0.57	862.19	16.31	39.15
K34	12.88 ± 0.51	718.02	13.59	32.61
K35	21.64 ± 0.67	1184.05	22.40	53.77
K36	15.83 ± 0.57	874.96	16.56	39.73
K37	21.00 ± 0.66	1150.00	21.76	52.22
K38	12.95 ± 0.52	721.74	13.66	32.78
K39	27.01 ± 0.74	1469.73	27.81	66.74
K40	21.08 ± 0.66	1154.26	21.84	52.42
K41	12.52 ± 0.51	698.86	13.22	31.74
K42	18.01 ± 0.61	990.93	18.75	45.00